2. Layout and buildings

The construction site is close to the internal highway of Pave and thus it is well connected by communication means. It is also located nearby the sites of three hospitals (San Matteo, Maugeri and Mondino) and the university campus and thus well placed to profit of clinical and research synergies that will be fundamental for the success of the CNAO initiatives. The buildings construction started in autumn 2005 and it is going to be completed in fall 2007.

The CNAO design is based on the following assumptions:

- the Centre will be devoted to the treatment of deep-seated tumours (up to a depth of 27cm of water equivalent) with light ion beams (proton, carbon ions and others) and to clinical and radiobiological research;
- the full-size CNAO will have 5 treatment rooms (3 rooms with fixed beams and 2 rooms with gantries) and one experimental room. For the first phase (CNAO - Phase 1) 3 treatment rooms will be equipped with 4 fixed beams, three horizontal and one vertical and one experimental room will be constructed (Figure 1).

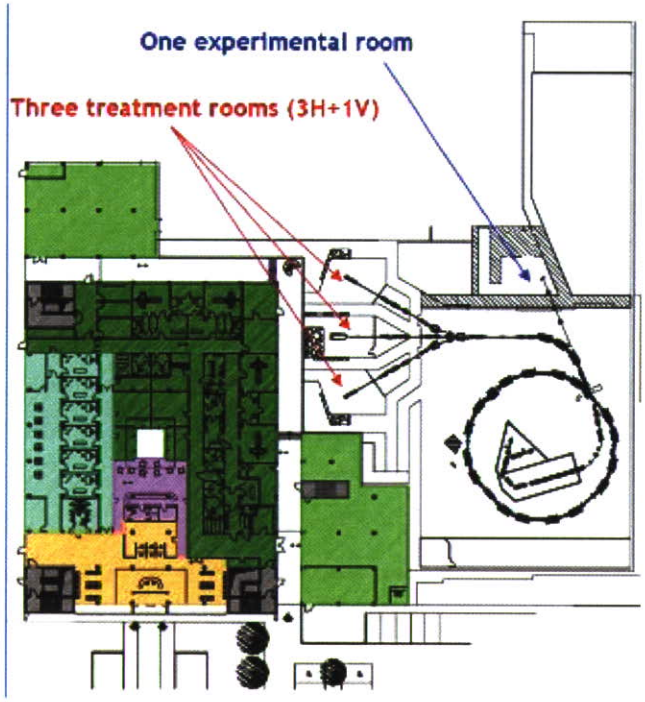

Fig. 1. Layout of the CNAO underground level - Phase 1.

The CNAO buildings develop on four levels. The underground level hosts the accelerators and the treatment rooms. The surface level hosts the ambulatories for the first visit of the patients and the medical imaging devices; two CT-PET cameras, two CTs and one NMR could be installed in the CNAO. These devices will permit the construction of the individual treatment planning for each patient. The first level is occupied by the offices of the personnel, the administration and also the spaces and the laboratories serving the experimental area. A direct connection between these areas and the experimental room is realised. The second floor occupies only half of the surface and it hosts a conference room, some smaller meeting rooms and also the direction offices. The flux of patients, personnel and public have been carefully studied in order to optimise the layout and to guarantee a quality of life that takes into account the needs of the various typology of people.

3. High Technology

The high technology design has been driven by the clinical requirements of the therapeutical beams, specified in Table 1.

Beam particle species	p, C^{6+}, (possibly He^{2+}, Li^{3+}, Be^{4+}, B^{5+}, O^{8+})
Beam particle switching time	≤ 10 min
Beam range	1.0 g/cm^2 to 27 g/cm^2 in one treatment room 3 g/cm^2 to 27 g/cm^2 elsewhere Up to 20 g/cm^2 for O^{8+} ions
Bragg peak modulation steps	0.1 g/cm^2
Range adjustment	0.1 g/cm^2
Adjustment/modulation accuracy	≤± 0.025 g/cm^2
Average dose rate	2 Gy/min (for treatment volumes of 1000 cm^3)
Delivery dose precision	≤± 2.5%
Beam axis height (above floor)	150 cm (head and neck beam line) 120 cm (elsewhere)
Beam size[1]	4 to 10 mm FWHM for each direction independently
Beam size step[1]	1.0 mm
Beam size accuracy[1]	≤± 0.2 mm
Beam position step[1]	0.8 mm
Beam position accuracy[1]	≤± 0.05 mm
Field size[1]	5 mm to 34 mm (diameter for ocular treatments) 2×2 cm^2 to 20×20 cm^2 (for H and V fixed beams)
Field position accuracy[1]	≤± 0.5 mm
Field dimensions step[1]	1 mm
Field size accuracy[1]	≤± 0.5 mm

[1] At isocentre or, for fixed beam, at normal treatment distance.

Table 1. Clinical performance specifications for the CNAO.

The clinical requirements have been defined by radiotherapists and medical physicists and have been discussed in detail within the international medical community. The basic design of the CNAO accelerator and lines has been hosted at CERN in the frame of the Proton-Ion Medical Machine Study (PIMMS), from 1996 to 1999 [1].

In order to translate the clinical requirements into a machine design for high-precision scanning, several accelerator design choices have been made during the PIMMS design. Some are listed below:

- application of emittance dilution at injection;
- use of a uniform, wide momentum, medium transverse emittance beam for extraction;
- use of the momentum-amplitude selection type of extraction with the Hardt Condition;
- use of a betatron core for accelerating the beam into the resonance;
- use of an rf empty bucket to channel the beam into the resonance;
- use of the bar-like shape in phase space of the extracted beam.

This concept design has been fully engineered, first by TERA and then by CNAO/INFN (with the help of GSI for the Linac, CERN for the special magnets - septa and kickers, University of Pave and LPSC/IN2P3 Laboratory of Grenoble for the betatron core). The final design now appears as shown in Figure 2.

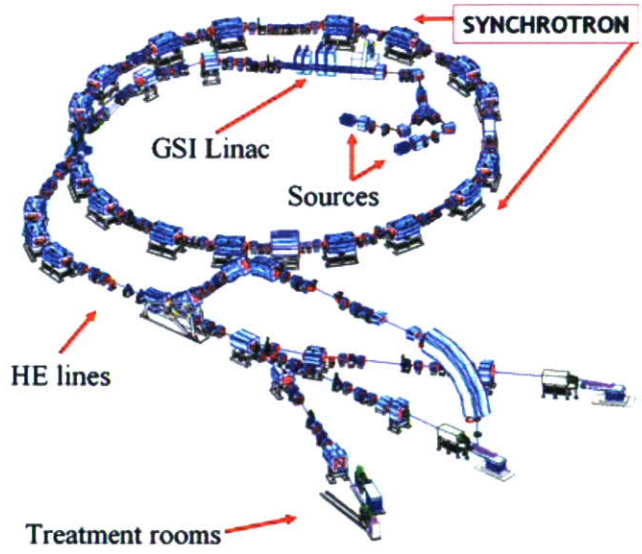

Fig. 2. Layout of the CNAO accelerators and beam transport lines.

Other important features have been added to the original PIMMS design:

• adoption of a single injector linac, designed by GSI and identical to the one used for the Heidelberg facility; the linac is suited for both protons and light ions acceleration;

• compact design of injection (inside the ring) and extraction beam transport lines (switching magnet concept);

• adoption of the multi-turn injection scheme;

• possibility to add in a second phase other treatment rooms with gantries without disturbing the routine medical activities.

A virtual tour of the beam lines and accelerator allows a brief presentation of the features of this optimised medical machine system. It has to be preliminarily underlined that the choices done for each device have taken into account the necessity to operate in a hospital based environment, the must of reaching an high operating efficiency (above 95%) and the satisfaction of basic requirements such as safety, reliability and maintainability have been the driving concepts of the CNAO design. CNAO will start activity with two identical ECR sources. The sources are already installed and preliminary measurements have been performed in May 2007. Figure 3

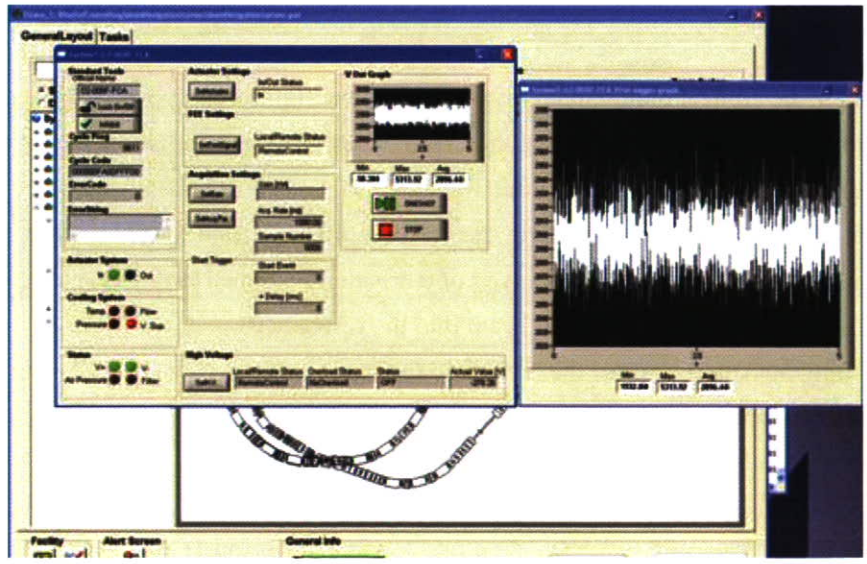

Fig. 3. First ion beam measured at the source exit with a Faraday cup.

shows the current of He3 measured with a Faraday cup.

The layout of the LEBT (Low Energy Beam Transfer) lines is designed in order to switch from one source to the other on a pulse to pulse basis. A spectrometer (90 degree bending) is placed downstream each source and a Faraday cup allows the routine setting up of the source and the related portion of LEBT before the beam utilization. This arrangement is very compact and allows the insertion of the source, LEBT and linac inside the synchrotron ring. The linac is composed of an RFQ and an IH-structure coupled together. It is identical to the one built for the Heidelberg project and it is being built under the technical supervision of GSI. The RFQ accelerates particles from 8 keV/u to 400 keV/u; the construction has been completed and it has been tested in July 2006 with the final power amplifier. The IH has been completed, vacuum tested and RF characterised at the beginning of 2007 at GSI. It accelerates the beams from 400 keV/u to 7 MeV/u.

The Medium Energy Beam Transfer line (MEBT) transports the beam from the stripping foil to the injection point in the synchrotron. In MEBT a final selection of the ion specie is made to avoid beam contamination with particles that before stripping have the same A/Q as the desired one. The CNAO synchrotron is made by two symmetric achromatic arcs joined by two dispersion free straight sections. The dispersion free sections host the injection/extraction region, the resonance driving sextupole and the RF cavity. The total length of the ring is approximately 78 m and accelerates particles till a maximum energy of 400 MeV/u, with a repetition rate of 0.4 Hz. The total bending of 360° has been divided in 16 identical dipoles powered in series. The focusing action is provided by 24 quadrupoles grouped in three families and the chromaticities are controlled by four sextupoles grouped in two families. A fifth sextupole is used for the third integer resonance excitation. Orbit correction is guaranteed by 20 steering magnets. The vacuum system, the beam diagnostics, the RF cavity, the special magnets for injection and extraction and the fast magnets for bumps and abort of the beam, the ring quadrupoles, sextupoles and correctors and the ancillary equipments (supports, cooling connections, alignment devices and so on) are already in Pave and partially installed. The four HEBT (High Energy Beam Tranfer) lines transport the extracted beam to the three treatment rooms. The HEBT dipole magnets are identical to the synchrotron magnets and this increases flexibility and reliability, reducing costs. The compact design is based on a switching magnet that is selecting the horizontal line to be used for treatment. An intrinsic safety aspect has been included in the HEBT design: interlaced with the first three dipoles of the extraction lines, a beam chopper has been installed. The chopper is composed by four fast dipoles powered in series with a +1, -1, -1, +1 scheme. This creates an orbit bump that brings the beam out of a dump at the start of the irradiation. Because of symmetry the beam stays on target also during the up and down ramps. The chopper intervention time is shorter than 260 microseconds to keep the dose delivered during intervention below 2.5% of the voxel dose. All the lines are equipped at the end with a pair of scanning magnets which allow scanning over an area of 200 mm x 200 mm.

Before the end of HEBT monitoring system is inserted that makes the link between the machine operation and the patient treatment. This device measures twice the intensity, the profile and the position of the pencil beam during the active irradiation of the target. The monitoring is the master of the treatment: it steers the scanning magnets and determine the completion of a treatment irradiation. The final version of the monitoring has been successfully tested both with protons and carbon ions. Other key features necessary to take advantage of the high spatial precision of hadrontherapy are an accurate individuation of the target and a precise and reproducible patient set-up. Treatments will be performed with patients immobilized on a couch or on a chair that will be docked to a state-of the art 6 degrees of freedom mobilization device. Set-up verification will be performed with orthogonal KV images of diagnostic quality. Additionally optoelectronic systems with markers detection and surface detection capability will be used. CNAO aims to have a high patients through-put. Design

has specifically addressed this issue and dedicated positioning rooms have been built (*Computed Assisted Positioning in Hadrontherapy*, CAPH rooms). Patients will be positioned on the couch (or on the chair) inside the CAPH rooms and then carried in the treatment room on a trolley predisposed for docking with the mobilization device, thus realizing a time optimization through a pipeline approach.

4. Clinical Activity

Protontherapy is considered the elective treatment for skull-base chordoma and chondrosarcoma, for uveal and choroidal melanoma and for paraspinal tumors. It has been used with promising results in a wide range of other diseases including bone and soft tissues sarcomas, HCC, NSCLC, CNS malignancies, head and neck tumors, pediatric tumors, prostatic adenocarcinoma and rectal cancer recurrence [3,4,8]. Experiences with carbon ions are still more preliminary, but results have been extremely encouraging in chordoma and chondrosarcoma, salivary gland tumors, sarcomas, HCC, NSCLC, advanced head and neck cancers, mucosal melanoma, recurrent rectal carcinoma, advanced uterine ceric carcinoma, bladder cancer, and prostate cancer [2,6,7,9]. CNAO will be able to use both protons and carbon ions [5]. At regime it will devote 80% of the time to ions and the remaining 20% to protons. CNAO activity is designed to reach regime in three years with two eight hours shifts from Monday to Friday. A workflow analysis has been performed and has shown that the facility will be able to deliver about 20 thousands treatment sessions per year. Hadrontherapy, and especially CIRT (Carbon Ion Radio Therapy), has shown a costant trend toward hypofractionation. At HIMAC (Japan) the mean number of fractions per patient is at present 13 and is still decreasing. At CNAO treatments will be carried out not only as exclusive therapy, but also as a boost after photons RT. It is estimated that about 3.400 patients per year will be treated at CNAO at regime. This number of patients is clearly inferior to the number of potential indications. There is therefore the need to define selection criteria to deliver hadrontherapy to patients that are more likely to benefit from it. To achieve this goal CNAO foundation have individuated seven groups of diseases that are considered at higher priority: lung tumours, liver tumours, sarcomas, head and neck tumours, eye tumours, central nervous system lesions and paediatric tumours. A disease specific working group has been created for each of these diseases under the leadership of a physician with recognized expertise in the field. Each working group is composed of radiation oncologists, medical oncologists, surgeons, diagnostic radiologists and organ specialists. The working groups have analyzed the literature and have produced documents with recomandations on tentative indications for trials to be conducted at CNAO. Special care has been taken to consider also alternative available treatments in the effort to propose hadrontherapy to those patients for whom it is reasonable to expect a significant advantage. A central board has been established to review documents written by the working groups and will eventually produce protocols for the trials that will start next year. Recently, two more working groups are being set-up on gynecological malignacies and on digestive cancers (pancreatic and rectal tumors). Another key issue for CNAO is to ensure a correct patient referral. CNAO will be the only carbon ion facility in Italy and therefore its basin will be the whole nation (besides foreign patients).

The clinical protocols will be submitted to the Ethical Committee and then presented to the Health Ministry in order to obtain the clinical authorizations to treat patients.

To allow a rational use of the facility it is mandatory to establish a close network with other oncological centers. For the near future CNAO will make the treatment protocols widely available to health providers, and will create specific tools for a quick patient referral (also employing approaches). A close cooperation with oncological centers and primary care provider is needed also to coordinate staging, follow-up (to be done mostly at the referring center) and treatment to be done at CNAO. An even closer cooperation will be necessary when

hadrontherapy is used within a multimodality treatment approach. An international cooperation has already started with the three European carbon ions centers foreseen (HIT, MedAustron, ETOILE) within the framework of the European project ULICE. This project aims at performing multicentric trials and at establishing a shared database of all treated patients.

5. Acknowledgements

The authors wish to thank the colleagues of CNAO Foundation and the collaborating institutes: thanks to their efforts the CNAO is becoming reality.

6. References

1. Badano L., Rossi S. et al.: Proton-Ion Medical Machine Study (PIMMS), Part I and II, CERN/PS 1999-010 DI and CERN/PS 2000-007 DR, Geneva.

2. Auberger T., Debus J., Gerard JP., Orecchia R., Potter R., Remillieux J., Ringborg U., Wambersie A.: Hadrontherapy with carbon12: radiotherapy of the near future. Radiother Oncol 2004; 73(Suppl 2):i-ii.

3. Jereczek-Fossa B.A., Krengli M, Orecchia R.: Particle beam radiotherapy for head and neck tumors: radiobiological basis and clinical experience. Head Neck 2006; 28(8):750-60.

4. Krengli M., Liebsch N.J., Hug E.B., Orecchia R.: Review of current protocols for protontherapy in USA. Tumori 1998; 84(2):209-16.

5. Krengli M., Orecchia R.: Medical aspects of the National Centre For Oncological Hadrontherapy (CNAO-Centro Nazionale Adroterapia Oncologica) in Italy.Radiother Oncol 2004; 73 (Suppl 2):S21-3.

6. Orecchia R., Fossati P.: Role of carbon ion therapy for stage I NSCLC using a regimen of four fractions over week. J Thorac Oncol 2007; 2(10): 887-8.

7. Orecchia R., Krengli M., Jereczek-Fossa B.A., Franzetti S., Gerard J.P.: Clinical and research validity of hadrontherapy with ion beams. Crit Rev Oncol Hematol 2004; 51(2): 81-90.

8. Orecchia R., Krengli M.: Number of potential patients to be treated with proton therapy in Italy. Tumori 1998; 84(2): 205-8.

9. Orecchia R., Zurlo A., Loasses A., Krengli M., Tosi G., Zurrida S., Zucali P., Veronesi U.: Particle beam therapy (hadrontherapy): basis for interest and clinical experience. Eur J Cancer 1998; 34(4): 459-68.

New Carbon Therapy Facility at Gunma University

Satoru YAMADA*, Tatsuya OHNO, Ken YUSA and Mutsumi TASHIRO

Gunma University Heavy Ion Medical Center,
3-39-22 Showa, Maebashi, Gunma 371-8511, JAPAN.

*Corresponding; satoru@showa.gunma-u.ac.jp

1. Introduction

In Japan, more than 300,000 patients are killed by cancer every year, and the number is increasing rapidly year by year. It is a top priority of the Japanese Government to protect the public against the spread of cancer. Clinical trials were initiated with high energy carbon beams obtained from HIMAC1) at National Institute of Radiological Sciences, NIRS, in 1994. Accumulating clinical results of more than 3,000 patients at HIMAC, it has been made clear that carbon therapy is very much effective in curing human cancers[2].

We have six working particle therapy facilities in Japan. Only one facility, however, can provide 400 MeV/u carbon ions, whereas 4 facilities provide proton beam only and the last facility at Hyogo can accelerate both protons and 320 MeV/u carbons.

In order to expand carbon therapy throughout the country, it is strongly desired to reduce construction and operation costs of an accelerator system. NIRS has carried out design and R&D studies to respond these demands. Gunma University has been collaborating on these studies since 2004. The new therapy facility at Gunma University will be the first full scale model of the design and R&D studies.

2. New Facility at Gunma-University Heavy-Ion Medical Center

Based on clinical statistics at HIMAC, a new carbon therapy facility is required to accelerate carbon ions up to 400 MeV/u. The maximum energy ensures 25 cm residual range in water and permit to treat prostate cancers through patient' s pelvis. Another important requirement of the new facility is to have two orthogonal beam lines directed toward the same isocenter. This beam line configuration is required in order to realize sequential beam irradiation from different directions with single patient position. First beam course and energy switching is also required to perform the sequential irradiation. Major specifications of the facility are summarized in table 1.

An accelerator of the facility consists of an all permanent magnet ECR type ion source, an RFQ linac, an IH linac with alternating phase focusing structure and a synchrotron ring followed by a high energy beam transport system. An averaged diameter of the synchrotron is about 20 m and will accelerate fully stripped carbon ions to an energy range from 140 to 400 MeV per nucleon. The facility will have three treatment rooms equipped with fixed beam ports and another irradiation room will be prepared for future developments. A wobbling technique will be adopted to obtain a uniform irradiation field of 15 cm square at maximum. The detailed design of the facility is based on design and R&D studies performed at National Institute of Radiological Sciences, NIRS. A layout of the new facility is given in Fig. 1.

Ions	Carbon ions only
Range	25 cm max. in water (400 MeV/u)
Field size	15 cm square
Dose Rate	5 GyE/min. ($1.2x10^9$ pps)
Treatment Rooms	3 (H, V, H&V), No rotational gantries
Fourth Room	Prepared for future developments
Irradiation Technique	Single & Spiral Wobbling, Respiration gated

Table 1: Major Specification of Gunma University Carbon Therapy Facility

3. Design and R&D Studies at NIRS

An ion source is an ECR type and developed at NIRS[5]. Both ring and sextupole magnets are made of NdFeB type permanent magnet. Magnetic filed is as high as 1.1 T at the surface of the magnets. Microwave frequency is made variable and chosen at around 10 GHz. An ion intensity of more than 300 e?A is obtained stably for C^{4+} ions with an extraction voltage and microwave power of 30 kV and 300 W, respectively.

An injector linac consists of a conventional four vane type RFQ linac followed by an interdigital H type linac with an alternating phase focusing structure, APF-IH[6), 7)]. An operation frequency of injector linac is chosen at 200 MHz, and an inside diameter of the linac tanks are about 35 cm. The maximum surface field is chosen to be 24 MV/m and 1.6 times larger than Kilpatrick' s value. This rather low value is adopted to keep electric breaking down risks to be extremely low level. During designing process of the APF-IH linac, we constructed a low power model cavity in order to check reliability of a 3-D computer code for calculation of rf characteristics of a cavity. A computer code Microwave Studio excellently reproduces experimental results.

A test stand which was designed to accelerate C^{4+} ions from an ECR source up to an energy of 4 MeV/u with RFQ and APF-IH linacs was developed at NIRS and beam tests were successfully performed. A photograph of the test stand is given in Fig. 2. Measured values of a beam energy, an energy spread, beam emittances very well reproduced calculated values.

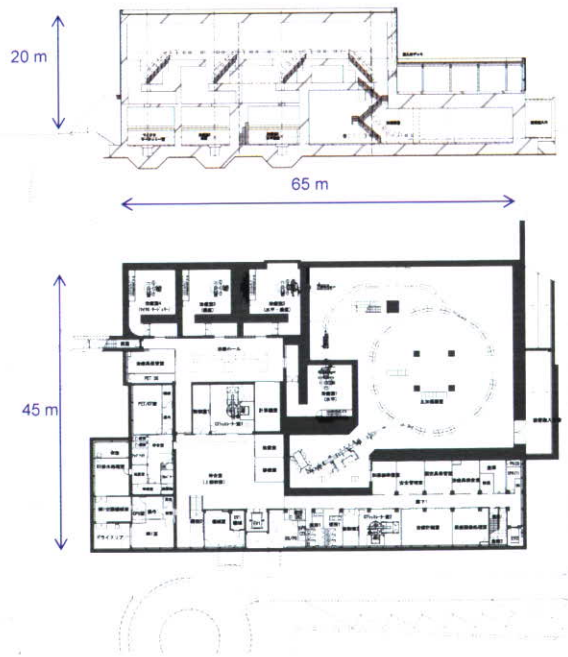

Fig. 1: A layout of the new facility.

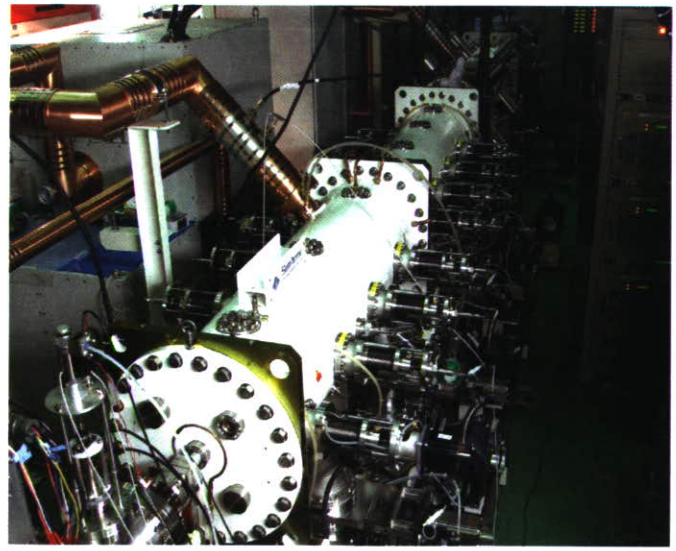

Fig. 2: A photograph of a test stand for an IH-APF linac.

An rf cavity loaded with Co based amorphous cores was developed for a synchrotron[8]. A shunt impedance of the cavity exceeded 300 Ω in a wide frequency range of 0.4 to 7 MHz without any tuning system. A new technique was applied in a cooling system of the amorphous cores: a cooling plate was adhered to only one side of the core to avoid making electric short paths across the core. The new cooling technique works very well without reducing shunt impedance of the cavity.

In order to increase beam utilization efficiency, a spiral wobbling technique was developed[9]. It requires about 1 minuet to paint whole irradiation field uniformly with rather small beam spots comparing with conventional single wobbling technique. The beam efficiency of around 45% is obtained with the spiral wobbling scheme, whereas single wobbling scheme gives only 17%. The calculated results have been reproduced very well by beam tests with high energy carbon beams from HIMAC.

4. Time Schedule of the Project

Based on the design and R&D studies described above, a new carbon therapy facility has been under construction at Gunma-University Heavy-Ion Medical Center. The construction started in February 2007 and will be completed in FY2008. Beam tests are scheduled in FY2009.

5. References

1) Y. Hirao, et al., Nucl. Phys. A538 (1992) 541c.

2) H. Tsujii, et al., Radiol. Sci. Vol.50, No.7 (2007) 5. (in Japanese)

3) K. Noda, et al., Nucl. Instr. Meth. A562 (2006) 1038.

4) K. Noda, et al., J. Rad. Res. 48 (2007) A43.

5) M. Muramatsu, et al., Rev. Sci. Instr. 76 (2005) 113304.

6) Y. Iwata, et al., Nucl. Instr. Meth. A566 (2006) 256.

7) Y. Iwata, et al., Nucl. Instr. Meth. A572 (2007) 1007.

8) M. Kanazawa, et al., Nucl. Instr. Meth. A566 (2006) 195.

9) M. Komori, et al., Jpn. J. Appl. Phys. 43 (2004) 6463.

Application of the Local Effect Model in Treatment Planning for Carbon Ion Therapy

Michael Scholz*, PhD, Thilo Elsässer, PhD, Michael Krämer, PhD

Gesellschaft fur Schwerionenforschung Dept. of Biophysics Planckstrasse
1 D-64291 Darmstadt Germany
*Corresponding: m.scholz@gsi.de

1 Introduction

The relative biological effectiveness (RBE) of charged particle beams depends on several factors such as particle type and energy, dose level and the cell or tissue type under consideration[1,2,3,4]. These systematic dependencies of the RBE have to be considered when using charged particle beams for therapy. As a consequence, RBE values are expected to be patient specific and can not be adequately represented by a single number for conversion of physical/absorbed dose to the biologically isoeffective dose.

For treatment planning, RBE values have to be estimated as precisely as possible. The facilities treating cancer patients with carbon ion beams are using different strategies. At HIMAC/Chiba, an experimentally oriented approach was developed. The shape of the isoeffective depth-dose profile is based on the precise measurements of RBE in-vitro. The clinical RBE value is then determined by a link to the clinical experience with neutron beams, which show similar radiobiological characteristics as carbon beams at the end of their penetration depth[5,6]. At GSI/Darmstadt, a modeling approach is used, which will be described in more detail below[7,8,9,10].

2 Modelling the increased effectiveness of charged particles

2.1 The Local Effect Model (LEM)

The biological optimization within treatment planning for the pilot project at GSI is based on the Local Effect Model (LEM). The principal assumption of the LEM is that the local biological effect, i.e. the biological damage in a small subvolume of the cell nucleus is solely determined by the expectation value of the energy deposition in that subvolume and is independent on the particular radiation type leading to that energy deposition. This is similar to the microdosimetric approach, but is applied to much smaller volumes compared to the µm-dimensions of microdosimetry. For a given biological object, all the differences in the biological action of charged particle beams should then be attributed to the different spatial energy deposition pattern of charged particles compared to photon irradiation, i.e. on track structure. Furthermore, for a given radiation type, any difference in RBE between different cell / tissue types should correspond to a difference also in the photon dose response curve.

The energy deposition pattern of charged particles is determined essentially by the secondary electrons (δ-electrons) liberated by the primary particle when penetrating matter. The average energy deposition as a function of the distance r from the trajectory, the radial dose profile, follows a $1/r^2$-law. According to the kinematics of the secondary electron emission, the maximum transversal range of the electrons is restricted and the corresponding track radius can be described by a power law of the form[11]:

$$R_{Max} = c \cdot E^{1.7} \qquad [1]$$

where c is a constant and E is the specific energy of the projectile. Details of the particular representation of the track structure and the radial dose profile as used in the local effect model are reported by Scholz et al.[10].

For the calculation of the biological effect of a given local dose deposition within the cell nucleus, the density of lethal events ν(d) can be defined as follows:

$$\nu(d) = \frac{\overline{N_{l,X}(d)}}{V_{Nucleus}} = \frac{-\log S_X(d)}{V_{Nucleus}} \qquad [2]$$

where $V_{nucleus}$ is the volume of the cell nucleus, d is the local dose, $N_{l,X}(d)$ represents the average number of lethal events produced by photon radiation in the nucleus by a dose d and $S_X(d)$ represents the photon dose response curve.

Given the complete local dose distribution according to the impact parameters of a given set of impinging ions, the average number of lethal events induced per cell by heavy ion irradiation can then be obtained by integration of the local event density $\nu(d(x,y,z))$

$$\overline{N_{l,Ion}} = \int \nu(d(x,y,z)\, dV_{Nucleus} = \int \frac{-\log S_X(d(x,y,z))}{V_{Nucleus}}\, dV_{Nucleus} \qquad [3]$$

This formula clearly demonstrates the theoretical link between the biological effect of photon radiation and ion radiation. The integrand is completely determined by the low-LET response of the object under investigation; the particle effect is 'hidden' in the inhomogenous local dose distribution $d(x,y,z)$. For a given pattern of particle traversals, the survival probability for a cell is then given by:

$$S_{Ion} = e^{-\overline{N_{l,Ion}}} \qquad [4]$$

Eq. [3] is the most general formulation of the local effect model; it does not rely on any particular representation of the photon dose response curve. It can be applied even if only numerical values of $S_X(D)$ are available. However, for practical reasons, we take the linear-quadratic approach for the description of the low-LET dose response curve. The average number of lethal events can then be identified with:

$$\overline{N_{l;X}} = \log S_X(D) = \alpha_X D + \beta_X D^2 \qquad [5]$$

A modified version of the linear-quadratic approach is used, since for many biological objects a transition from the shouldered to an exponential shape of the dose response curve is observed at high doses. This transition is described by a parameter Dt, representing the transition dose to the exponential shape with slope , $S_{max} = \alpha + 2\beta D_t$, so that the dose response is finally given by:

$$S_X(D) = \begin{cases} e^{-(\alpha_X D + \beta_X D^2)} & : D \le D_t \\ e^{-(\alpha_X D_t + \beta_X D_t^2 + s_{max}(D - D_t))} & : D > D_t \end{cases} \qquad [6]$$

In general, the dose D_t cannot be directly derived from experimental data, since survival curves can be measured only down to 10^{-3} for most mammalian cell lines; D_t represents thus a semi-free parameter of the model. The value of D_t can be estimated, however, based on the finding, that differences in sensitivity between different

cell lines are expressed in general in a variation of the initial slope (α-term), whereas the β-term and thus the final slope S_{max} are very similar. In general, values for S_{max} in the order of 2 Gy^{-1} and the corresponding value for D_t - resulting from the particular α- and β-values - allow consistent descriptions of the experimental data.

In order to perform the numerical integration given in eq.[3] for a random distribution of particle traversals, a small grid has to be used in order to cope with the rapid, position-dependent variation according to the $1/r^2$-distribution of the radial dose profile. This leads to unacceptable computing times not compatible with the needs of treatment planning. Therefore, approximation procedures have been developed. The approximations are related to the estimation of the β-parameter of the dose response curve; the α-parameter can be always calculated exactly according to eq. [3], since the initial slope corresponds to the effect at very low doses and thus fluences. In this case, the dose response is defined by single particle effects, and no overlap of contributions from different particles has to be taken into account. A more detailed discussion would be beyond the scope of this report; details of the approximations are reported by Scholz et al.[10] and Krämer and Scholz[12].

2.2 Comparison with experimental data

Fig. 1 compares RBE(LET) relationships for 2 different cell lines calculated according to the original LEM as reported by Scholz et al.[10] and the optimized LEM as described by Elsässer and Scholz[13] with experimental data for carbon ion irradiation.

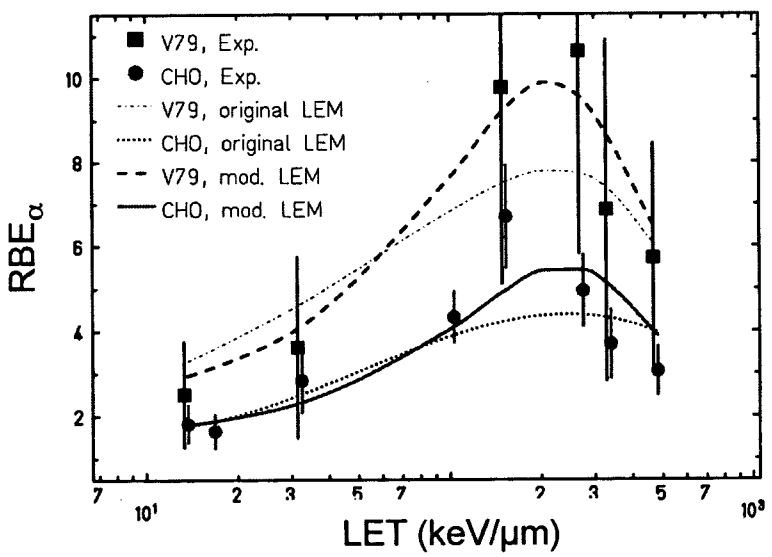

Fig. 1:The RBE is investigated for two different mammalian cell lines (V79 and CHO cells) after carbon-ion irradiation. The modified local effect model (thick lines) agrees better with the experimental data[3] than the classical local effect model (thin lines). The corresponding data for the X-ray survival curve of CHO cells are α=0.228 Gy^{-1}, β=0.02 Gy^{-2}, D_t=40 Gy (old) and D_t=9.5 Gy (modified). Input parameters for V79 cells are α=0.093 Gy^{-1}, β=0.026 Gy^{-2}, D_t=30 Gy (old) and D_t=7.5 Gy (modified), respectively.

A good agreement between model prediction and experimental data is observed in particular for the modified LEM including cluster effects, and the higher RBE for V79 cells as compared to CHO cells is well reproduced. The RBE apparently correlates with the repair capacity of the cell, as reflected by the increasing width of the shoulder of the photon dose response curves.

2.3 Transfer to complex tissues in-vivo.

Fig. 1 demonstrates, that different cell types are characterized by different RBE values, and the same is expected to hold true also in the in-vivo and clinical situation. Therefore, normal tissues and tumor tissues might show different RBE values, but also within the groups of normal and tumor tissues a significant variation of RBE can be expected. Therefore, the question arises how to transfer the RBE values determined in-vitro to the in-vivo or clinical situation.

The local effect model as described above is based on the knowledge of the photon dose response curve. However, representative photon survival curves are not available for all tissues under consideration, and even if available, the correlation between cell survival and the clinically relevant tissue response remains unclear, at least on a quantitative level. Therefore, we have to ask which characteristic of the photon dose response curve is the most relevant for the determination of RBE.

According to eqs. [3] and [5], the nonlinearity of the photon dose response curve is a prerequisite for the prediction of RBE values greater than one. If the photon dose response curve is purely exponential, RBE is expected to be equal to one. In contrast, in the case of a shouldered x-ray dose response curve, a higher effectiveness is expected. According to that systematic, when comparing different biological systems with different photon dose response curves, for a given particle type and energy the RBE should increase with the slope ratio

$$r = s_{\max}/\alpha = 1 + 2\frac{\beta}{\alpha}D_t \qquad [7]$$

since the highest effectiveness of the very high local doses in the center of the charged particle track is determined by the final slope of the photon dose response curve.

Fig. 2 demonstrates this dependence of RBE on the slope ratio of the photon dose response curve by means of calculated RBE values as a function of dose for irradiation in an extended Bragg peak. In Fig. 2a, constant values for α/β and Dt and thus also for r are assumed, but the absolute values of α and β are varied by a factor of 50. Despite this large variation, the expected RBE values only show minor differences. In sharp contrast, for a variation of the slope ratio r, expressed here through the corresponding variation of the α/β-ratio and simultaneous adjustment of Dt to achieve the same final slope of $2Gy^{-1}$, an extreme variation of RBE is expected (Fig. 2b). In line with the qualitative description above, the RBE is highest in the case of a small α/β-ratio.

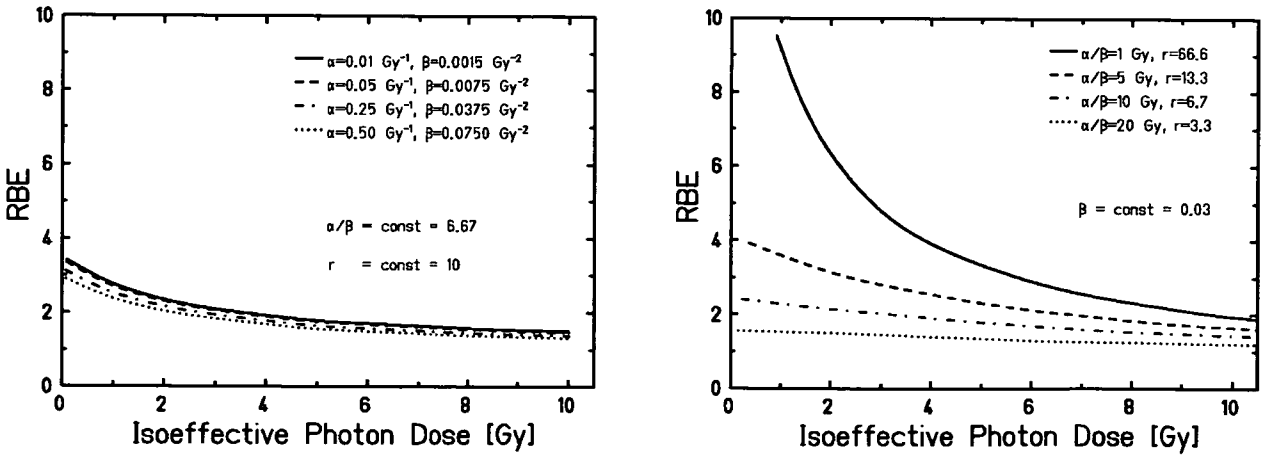

Fig. 2:Comparison of predicted RBE values in the middle of a 4cm extended Bragg peak. (a): Constant α /β-ratio, variation of absolute values of α and β. (b): Constant β, variation of α and thus α/β.

These findings are in agreement with other reports, suggesting that radioresistant cell lines (characterized by a small α/β ratio) in general show a more significant enhanced RBE than sensitive cell lines[14,15].

The systematic mentioned above opens the application of the LEM also to complex normal tissue effects. This is done by drawing an analogous conclusion: if two biological endpoints are characterized by the same α /β-ratio of the photon dose response curve, they should also show the same RBE for a given type of radiation. Since α/β-ratios are known for many normal tissues, these can be used to estimate the RBE. I.e., the model calculation is performed using a photon survival curve, having the same α/β-ratio as the tissue endpoint under consideration, and then assuming that both the survival curve and the tissue endpoint will show the same RBE at a given dose level. Therefore, if no detailed information about the absolute values of α and β for the tissue under consideration are available, RBE values for treatment planning are based on the α/β-ratio for the specific tissue and endpoint under consideration.

3 Application in treatment planning

It has been shown, that the LEM is able to predict dose response curves for endpoints in vitro, in-vivo and also for clinical data with good precision[16]. It has been implemented in the biological optimization module of the treatment planning procedure TRiP[12,17,18] for the carbon ion therapy project at GSI. Due to the tissue dependence of RBE, the biological characteristic of each tissue relevant for the therapeutic situation has to be specified. According to the principles of the model as described above, the biological characteristic with respect to radiation quality is essentially determined by the α/β-ratio for conventional photon radiation of the tissue under consideration and the value of D_t.

Frequently, values of α/β =10Gy are quoted for early responding normal and tumor tissues and α/β=3 Gy for late responding normal tissues. However, it is not appropriate to use these values for the purposes discussed here. In particular the value of α/β=10Gy does not reflect the situation for the tumor entities, which are expected to mostly benefit from the high-LET effect, and thus more realistic values should be used as described below.

In any case the photon parameters specific for the tissue and endpoint under consideration should be used for the estimation of RBE. Consequently, different parameters have must be applied in general for different tissues, and similarly different parameters have to be used when calculating the RBE for early and late effects in a given normal tissue, respectively. Ideally, α/β derived from clinical data would be appropriate. If these are not available, the corresponding data from representative in-vivo studies should be used, and if those are not available, *in-vitro* experiments might help to deduce the photon sensitivity parameters.

Up to now, mainly chordomas, chondrosarcomas and adenoid cystic carcinomas have been treated with carbon ions within the GSI pilot project. Since the α/β-values cannot be directly derived from clinical data for these rare tumors, the corresponding values have to be estimated based on other data. A very useful set of clinical data in that respect is the investigation of the growth characteristic of tumor metastasis in the lung as reported by Battermann et al.[19], showing a clear correlation of the photon sensitivity of the metastasis with the tumor volume doubling time. When this set of data is reanalyzed using the linear-quadratic model, it can be demonstrated that the corresponding α/β-values decrease as a function of the tumor volume doubling time. Obviously, not only the sensitivity in general, but also the α/β-ratio depends on the tumor volume doubling time. According to this analysis, the α/β-ratio of slow growing tumors is consistent with values as low as 2 Gy, and is thus con-

siderably lower than the value assumed in general for tumor tissues and early responding tissues (α/β=10 Gy) For the treatments of chordomas and chondrosarcomas, the α/β-value for the tumor tissue is thus expected to be at least very similar to that of the surrounding normal tissue. For the brain tissue, an α/β-value of 2 Gy has been chosen in accordance with the knowledge from in-vivo irradiations e.g. of the spinal cord. Consequently, although the tissues are completely different in general, a similar characteristic has been assumed with respect to their response to photon radiation in terms of their α/β-ratio.

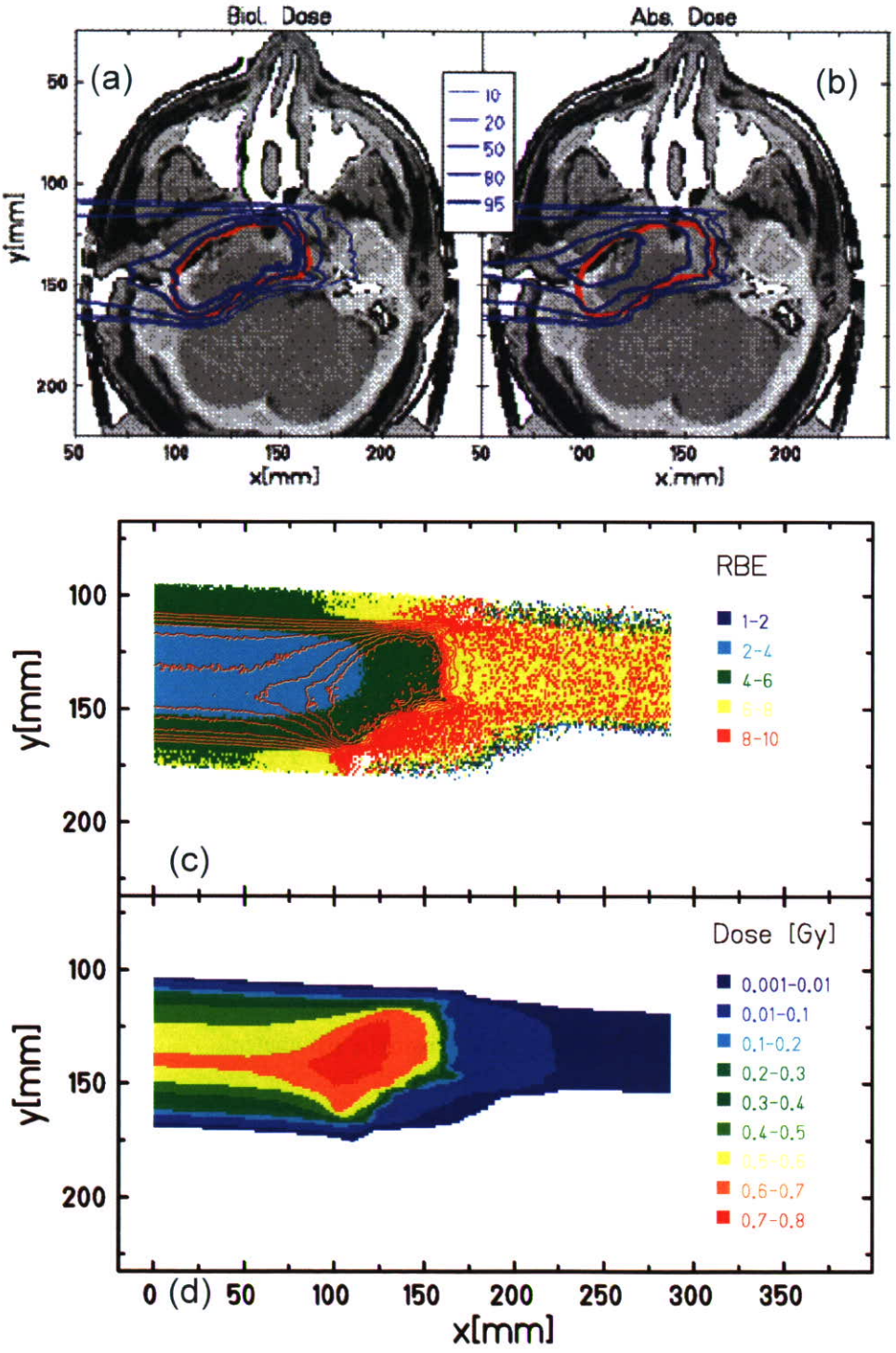

Fig. 3:Comparison of biological effective dose distribution (a) and absorbed dose distribution (b) for a typical treatment plan. The corresponding RBE-distribution in comparison to the absorbed dose distribution is shown in (c) and (d).

Fig. 3 shows an example for the distribution of RBE values for a typical treatment plan of a chordoma patient; the position dependent variation of RBE becomes clearly visible. In the TRiP treatment planning procedure also the dose dependence of RBE is fully reflected, and RBE values are always calculated exactly for the dose, which is actually applied at a given point in the treatment field. As a consequence, this dose dependence of RBE also contributes to the spatial variation of RBE: Since RBE increases with decreasing dose, comparably high RBE values are also expected at the boarder of the treatment field and beyond the distal end of the extended Bragg peak. Explicitly considering also the dose dependence of RBE represents an important difference to other approaches as they are applied e.g. at the HIMAC, where RBE values are usually considered at a fixed effect level, i.e. 10% survival.

The influence of the tissue composition is demonstrated in Fig. 4. The upper full line represents the isoeffective depth dose distribution for a homogenous biological characteristic with α/β=2 Gy throughout the whole irradiated volume. The arrow on the left side depicts the isoeffective dose for the induction of acute effects in the skin at the entrance port, based an α/β= 5.9 Gy; this value was derived from a reanalysis of the data reported by Hopewell[20]. According to the general systematic discussed already above, the isoeffective dose for skin reaction is significantly lower than the value for chordoma or late CNS tissue effects because of the higher α/β-ratio.

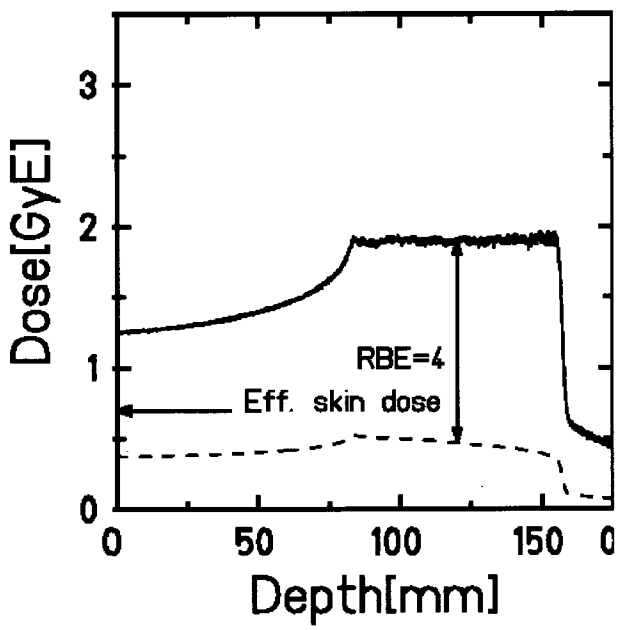

Fig. 4:Depth dose profiles (in a water-equivalent system) for a typical chordoma treatment. The full line indicates the isoeffective dose distribution based on α/β=2Gy; the arrow at the left side indicates the isoffective dose level for acute skin reactions based on α/β=5.9 Gy.

More precise information with respect to α/β-ratios is available for other tumor entities like e.g. prostate tumor. Although the debate about the precise α/β-value for prostate cancer is ongoing and the details are still under discussion, there is general agreement that the value is below 3 Gy and thus definitely lower than 10 Gy as typically assumed for other tumors. This low value makes prostate cancer a good candidate for ion beam treatment, because according to the systematic shown in Fig. 2 the RBE is expected to be high in this case.

In order to allow for a comparison with other treatment modalities like proton or advanced photon techniques like IMRT, which are mainly performed using a 2 Gy/fraction scheme, the differences in the fractionation

schedule have to be taken into account as well. So far, typical full carbon ion treatments at GSI have been performed using a 20 fraction schedule on 20 consecutive days without breaks at the weekend and an isoeffective fraction dose of 3 Gy, resulting in a total isoeffective dose of 60 Gy. (RBE values are in the order of 3 for these cases, so that the total absorbed dose is in the order of 20 Gy). The estimation of the fractionation effects requires the same α/β-values which are taken for the estimation of RBE values. For example, based on an α/β-value of 2 Gy, the isoeffective dose of 60 Gy in 20 fractions corresponds to a dose of approximately 75 Gy when given with a dose of 2 Gy per fraction.

4 Conclusions

The complex dependence of RBE on parameters such as particle type and energy, dose level and cell or tissue type require careful consideration in treatment planning for applications of charged particle beams in tumor therapy. For the precise quantitative description of these dependencies, models are required. An example of such a model, the local effect model (LEM) is described in this report. It has been tested by comparison with a wide variety of biological endpoints from in-vitro cell survival to tumor control probabilities from clinical studies.

An important feature of the approach presented here is, that it allows prediction of the response of a biological object to high-LET radiation from its response to low-LET radiation: for a given treatment field, the RBE is essentially determined by the photon sensitivity parameters α, β and Dt. Therefore, the experience with conventional photon treatment represents an important source for estimation of clinical RBE values.

5 References

1. Blakely, E.A., 'Biology of BEVALAC beams' In: Pion and heavy ion Radiotherapy: Pre-Clinical and Clinical Studies Skarsgard LD Ed. New York. (Elsevier Science Publishing Co, Inc.) 229-250 (1982)
2. Kraft, G., Radiobiological Effects of Very Heavy Ions: Inactivation, Induction of Chromosome Aberrations and Strand Breaks. Nucl. Sci. Appl., 3, 1-28 (1987)
3. Weyrather, W.K., Ritter, S., Scholz, M., Kraft, G., RBE for carbon track-segment irradiation in cell lines of different repair capacity. Int.J.Radiat.Biol., 75, 1357-1364 (1999)
4. Furusawa, Y., Fukutsu, K., Aoki, M. et al., Inactivation of aerobic and hypoxic cells from three different cell lines by accelerated 3He-, 12C- and 20Ne-ion beams. Radiat.Res. 154, 485-496 (2000)
5. Kanai T, Furusawa Y, Fukutsu K, et al., Irradiation of Mixed Beam and Design of Spread-Out Bragg Peak for Heavy-Ion Radiotherapy. Radiat. Res. 147, 78-85 (1997)
6. Kanai, T., Endo, M., Minohara, S. et al., Biophysical characteristics of HIMAC clinical irradiation system for heavy-ion radiation therapy. Int. J. Radiat. Oncol. Biol. Phys. 44, 201-10 (1999)
7. Scholz, M., Kraft, G. Calculation of heavy ion inactivation probabilities based on track structure, x-ray sensitivity and target size. Radiat. Prot. Dosim. 52, 29-33 (1994)
8. Scholz, M., Kraft, G. Track structure and the calculation of biological effects of heavy charged particles. Adv. Space Res. 5-14 (1996)
9. Scholz, M. Calculation of RBE for normal tissue complications based on charged particle track structure. Bull. Cancer Radiother. 83 Suppl., 50s-54s (1996)
10. Scholz, M, Kellerer, AM, Kraft-Weyrather, W, Kraft, G. Computation of cell survival in heavy ion beams for therapy - the model and its approximation. Radiat. Environ. Biophysics 36, 59-66 (1997)
11. Kiefer, J., Straaten, H. A model of ion track structure based on classical collision dynamics. Phys. Med.

Biol. 31, 1201-9 (1986)

12. Krämer, M. and Scholz, M. Rapid calculation of biological effects in ion radiotherapy. Phys. Med. Biol. 51 (2006) 1959?1970
13. Elsässer, T. and Scholz, M., Cluster Effects within the Local Effect Model. Rad. Res., 167:319-329 (2007)
14. Suzuki M, Kase Y, Yamaguchi H, et al. Relative biological effectiveness for cell-killing effect on various human cell lines irradiated with heavy-ion medical accelerator in Chiba (HIMAC) carbon-ion beams. Int J Radiat Oncol Biol Phys 48, 241-50 (2000)
15. Weyrather, W.K., Kraft, G. RBE of carbon ions: Experimental data and the strategy of RBE calculation for treatment planning. Accepted for publication in Radiotherapy and Oncology (2003)
16. Scholz, M., Matsufuji, N., Kanai, T. Test of the local effect model using clinical data: tumour control probability for lung tumours after treatment with carbon ion beams.Radiat Prot Dosimetry. 2006;122 (1-4):478-9
17. Krämer, M, Jäkel, O, Haberer, T. et al.. Treatment planning for heavy-ion radiotherapy: physical beam model and dose optimization. Phys. Med. Biol. 45, 3299-3317 (2000)
18. Krämer, M and Scholz, M. Treatment planning for heavy-ion radio therapy: calculation and optimization of biologically effective dose. Phys. Med. Biol. 45, 3319-3330 (2000)
19. Battermann JJ, Breur K, Hart GA, van Peperzeel HA. Observations on pulmonary metastases in patients after single doses and multiple fractions of fast neutrons and cobalt-60 gamma rays. Eur J Cancer. 17 (1981) 539-48
20. Hopewell JW, van den Aardweg GJ. Studies of dose-fractionation on early and late responses in pig skin: a reappraisal of the importance of the overall treatment time and its effects on radiosensitization and in-complete repair. Int J Radiat Oncol Biol Phys. 1991 Nov;21(6):1441-50.

NIRS Methods of Specifying Carbon Ion Dose

Naruhiro Matsufuji*, Yuki Kase and Tatsuaki Kanai

Radiation Effect Research Team, Research Center for Charged Particle Therapy,
National Institute of Radiological Sciences

*Corresponding: matufuji@nirs.go.jp

1. Introduction

Many studies in the field of radiobiology have revealed that the clinical or biological effectiveness of heavy charged particles is a variable quantity. It results in that a physical dose is still a primary quantity to be controlled in carbon ion radiotherapy like as other conventional radiations, however, a kind of modification is indispensable for therapeutic purpose. Here, RBE is introduced as a tool to account for the modification. However, RBE depends on various physical parameters, as mentioned above. Primarily, RBE of a heavy ion beam gradually increases as the LET by the beam increases, reaches its maximum and then decreases. In addition, the RBE curve is known to show a different behavior for different ion species, fractionation schedules, or even dose levels. Even if these physical conditions are identical, RBE also varies as a function of biological parameters such as the type of tissue or cell, oxygenic conditions, endpoint of interest, and so on. The enormous complexity of the RBE determination hinders itself from being fully understood even at this moment. At HIMAC, unproven behaviors of factors such as dose dependency or tissue-specific response to carbon ions are kept constant in order to ascertain them from clinical outcomes.

2. Materials and Methods

At first, fragmentation of monoenergetic carbon ions in a patient' s body is estimated with a simulation code HIBRAC [1]. Dose-averaged LET value is deduced at each depth from the calculated LET spectra. HSG, cell line from human salivary grand tumor, was chosen as a representative of various cell lines due to its moderate radiosensitivity. Dose-survival relationships of the HSG to carbon ions of various incident energies are characterized with 2 parameters, α and β, by the LQ model. SOBP is designed to achieve flat survival probability (10%) on HSG entire SOBP region. Here, dose-averaging coefficients α and β are used for survival calculation at each depth regarding composition of the beam.

It is assumed that carbon beam is clinically equivalent to fast neutrons at the point where dose-averaged LET values is 80 keV/μm. Our enormous neutron therapy experience tells that neutron has clinical RBE of 3.0. Then, clinical RBE of carbon is also normalized to 3.0 at the point. Clinical SOBP shape is finally deduced by equally multiplying a fixed factor, the ratio between clinical- and biological RBE value at the point where dose-averaged LET is 80 keV/μm, to entire biological SOBP.

This scheme for the designing of clinical dose results in applying universal depth-dose distributions to all patients, independent of tumor type or dose level. The universal depth dose distributions are considered to be beneficial to clarify the clinical effectiveness of carbon ion radiotherapy through clinical trials when dose dependency or the difference of radiosensitivity among tumor type is not yet proven from the viewpoint that it contributes to reduce the number of free parameters. Fig. 1 schematically shows the method for determining the RBE at the center of the SOBP for clinical situations.

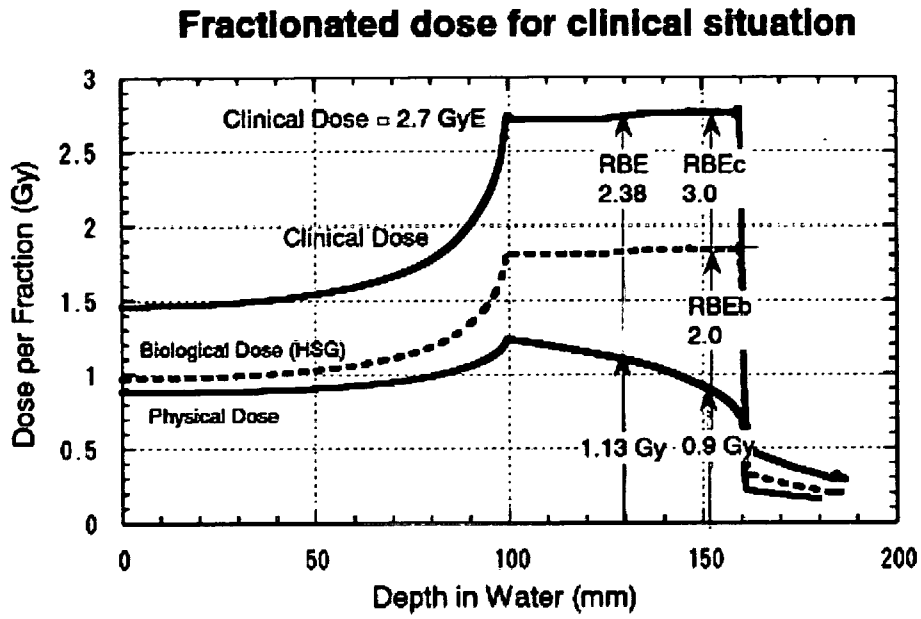

Fig. 1 Schematic method used to determine the RBE at the center of the SOBP for the clinical situation.

3. Results and Discussion

Verification of clinical RBE

We present here tumour control probability (TCP) analysis for non-small cell lung cancer (NSCLC) as an example of clinical results in terms of above-mentioned clinical RBE prescription scheme. Miyamoto et al. analyzed the clinical results of NSCLC treated by HIMAC beams [2]. They depict very conspicuous dose dependency of local control rate. The dose escalation study was performed with a treatment schedule of 18 fractions in 6 weeks. As to photon, Hayakawa el al. reported local control rate for NSCLC. In order to compare both results, the dose dependency of the TCP with the photon beam was fitted by the following formula [3];

$$TCP = \sum_i \frac{1}{\sqrt{2\pi}\sigma}\left\{-\frac{(\alpha_i-\alpha)^2}{2\sigma^2}\right\}\cdot\exp\left[-N\exp\left\{-n\alpha d\left(1+\frac{d}{\alpha/\beta}\right)+\frac{0.693(T-T_k)}{T_p}\right\}\right]. \quad (1)$$

α and β are coefficients of LQ model of cell survival curve. In the analysis, α and β values of HSG cells were used. σ is a standard deviation of the coefficient α, which reflects patient-to-patient variation of radiosensitivity. N is the number of clonogen in tumor (fixed value of 10^9 was used). n and d are total fraction number and fractionated dose, respectively. T (42 days), T_k (0 day) and T_p (60 days) are overall time for treatment, kick off time and average doubling time of tumor cells, respectively. Values used in the analysis are shown in brackets. The result is shown in fig. 2.